Numerical simulation of the effect of the Al molar fraction and thickness of an $Al_xGa_{1−x}As$ window on the sensitivity of a p^+–n–n^+ GaAs solar cell to 1 MeV electron irradiation

A.F. Meftah [a], N. Sengouga [a,*], A.M. Meftah [a], S. Khelifi [b]

[a] Laboratory of Metallic and Semiconducting Materials, Faculty of Science and Engineering, Mohamed Kheider University, B.P. 145, 07000 Biskra, Algeria
[b] Laboratory of Semiconductor Devices Physics, Physics Department, University of Béchar, P.O. Box 417, Béchar 08000, Algeria

ABSTRACT

In this paper numerical simulation has been used to predict the effect of the thickness and aluminium (Al) mole fraction of an AlGaAs layer, used as a window for a p^+–n–n^+ GaAs solar cell under AM0 illumination and exposed to 1 MeV electron irradiation. Such solar cells are used in satellites and undergo severe degradation in their performance due to induced structural defects. The irradiation-induced defects are modelled as energy levels in the energy gap of GaAs. To predict this effect, the spectral response is evaluated for different electron irradiation fluences for two types of cells. In the first a narrow $Al_{0.31}Ga_{0.69}As$ window is a small part of the p^+ layer while in the second type the whole window is an $Al_xGa_{1−x}As$ layer with a gradual Al mole fraction. The obtained results show that the $Al_xGa_{1−x}As$ window with a gradual Al mole fraction improves the resistance of the solar cell to electron irradiation especially in the short wavelengths range.

© 2009 Elsevier Ltd. All rights reserved.

1. Introduction

Photovoltaic based power sources for satellites require radiation resistant and high efficiency solar cells. Si, GaAs, InP and InGaP are exclusive materials that can meet both requirements because of their mature technology which can produce high quality materials as well as good doping control [1–4]. While Si offers the obvious advantage of more mature and relatively cheap technology, compound semiconductors have higher conversion efficiency and radiation resistance due to their higher absorption coefficient and direct larger energy band gap.

Among compound semiconductor materials, GaAs is commonly preferred for space applications because of its more advanced and cheaper technology, conversion efficiency and radiation resistance [1]. Unfortunately an all-GaAs solar cell suffers from carrier loss due to a high surface recombination velocity [5]. In order to reduce such loss a wide band gap surface layer of $Al_xGa_{1−x}As$ is placed on the top of a GaAs emitter to create a heterojunction solar cell [5,6]. The $Al_xGa_{1−x}As$/GaAs interface has minimal interface states owing to the small mismatch between AlAs and GaAs [5]. With a wide band gap layer, minority carriers in the emitter undergo an additional force which prevents their motion back to the cell's top surface. This increases the cell's open circuit voltage, collection efficiency and absorption at short wavelengths [5–7].

When exposed to cosmic particle irradiations such as electrons and protons, solar cells undergo significant deterioration in their performance. This constitutes a serious problem for the power supplies of satellites operating in orbits. The mechanism of irradiation-induced degradation has been widely studied [2–4,8–11]. Electron irradiation for example introduces simple intrinsic defects, i.e. vacancies and interstitials that give rise to energy levels (recombination centers and traps) in the semiconductor energy gap [4,8]. The prediction of the effect of irradiation is an essential step before solar cells are put into use.

Numerical simulation is a powerful tool to reach this objective. Many parameters can be varied to model the observed phenomenon. It can also offer a physical explanation of the observed phenomenon since internal parameters such as the electrical field, the recombination rate and the free carrier densities can be calculated.

In a previous work, numerical simulation is used to predict the effect of the electron irradiation on the output parameters of a homojunction GaAs solar cell, namely the short circuit current, the open circuit voltage, the efficiency and the fill factor [12]. In this

* Corresponding author. Tel./fax: +213 33 74 10 87.
E-mail address: nouredine_sengouga@yahoo.co.uk (N. Sengouga).

work numerical simulation is used to predict the effect of the $Al_xGa_{1-x}As$ layer thickness and composition in reducing the degradation of a p^+-$Al_xGa_{1-x}As/p^+$–n–n^+ GaAs solar by 1 MeV electron irradiation.

2. Numerical model

The simulation program developed is based on the Kurata method [13] which gives a one-dimensional numerical solution of the carrier transport problem in a p^+–n–n^+ solar cell. A stationary simultaneous solution of Poisson's equation and hole and electron continuity equations, approximated by a finite difference, is obtained. These equations are:

$$\frac{1}{q}\frac{dJ_n}{dx} + G(x) - U(x) = 0 \tag{1.a}$$

$$\frac{1}{q}\frac{dJ_p}{dx} - G(x) + U(x) = 0 \tag{1.b}$$

$$\frac{d}{dx}\left(\varepsilon_0\varepsilon_r(x)\frac{d\psi}{dx}\right) = -\rho(x) \tag{2}$$

Here ψ is the electrostatic potential, J_n and J_p are the electron and hole conduction current densities given, for variable composition devices, by [6,14]:

$$J_n = -\mu_n n\left(q\frac{d\psi}{dx} + \frac{d\chi}{dx} + \frac{k_BT}{N_c}\frac{dN_c}{dx}\right) + k_BT\mu_n\frac{dn}{dx} \tag{3.a}$$

and

$$J_p = -\mu_p p\left(q\frac{d\psi}{dx} + \frac{d\chi}{dx} + \frac{dE_g}{dx} - \frac{k_BT}{N_v}\frac{dN_v}{dx}\right) - k_BT\mu_p\frac{dp}{dx} \tag{3.b}$$

where χ, E_g, N_c, N_v, n and p are the semiconductor affinity, energy gap, effective densities of states in the conduction and valence bands, the electron density and the hole density respectively. All these quantities are evidently space dependent (along the x-axis). μ_n and μ_p are the electron and hole mobilities which are also space as well as doping densities dependent while their electric field dependency is neglected since the electric field in solar cells usually has small values (below critical fields for velocity saturation). q and k_B are the electronic charge and Boltzmann constants respectively. T is the absolute temperature, ε_0 is the permittivity of the free space and $\varepsilon_r(x)$ is the dielectric constant which is also space dependent for a heterojunction.

G is the generation rate which will be detailed in Section 3 (equation (12)), $\rho(x)$ is the space charge density given by:

$$\rho(x) = q\left(p - n + N_D(x) - N_A(x) \pm \sum_i N_i^{\pm}\right) \tag{4}$$

where $N_{A(D)}$ is the acceptor (donor) doping density, $N_i^{\pm}$ is the ionised ith defect density. Because of the sometimes confusing definitions of deep levels, Miller et al.'s definition [15] which states "an electron trap is neutral when occupied and positively charged when empty while a hole trap is neutral when occupied by holes and negatively charged when empty" is used.

$U(x)$ is the total recombination rate, which includes the Shockley–Read–Hall (SRH) recombination rate ($U_{SRH}(x)$), the radiative direct recombination rate ($U_{rd}(x)$) and the Auger recombination rate ($U_{Aug}(x)$). $U_{SRH}(x)$ is given by:

$$U_{SRH}(x) = \sum_i U_i(x) \tag{5}$$

where $U_i(x)$ are the recombination rate of the ith defect which is given by SRH (Shockley–Read–Hall) statistics as [16,17]:

$$U_i = \frac{(n \cdot p - n_i^2)}{\tau_{ni}(n + n_{1i}) + \tau_{pi}(p + p_{1i})} \tag{6}$$

where τ_{ni} and τ_{pi} are the minority carrier lifetime which are related to the defect's density N_i and capture cross-sections for electrons and holes σ_{ni} and σ_{pi} by $\tau_{ni} = 1/\sigma_{ni}v_{th}N_i$ and $\tau_{pi} = 1/\sigma_{pi}v_{th}N_i$, v_{th} is the thermal velocity supposed to be the same for electrons and holes for simplicity, n_i is the semiconductor intrinsic density and n_{1i} and p_{1i} are the electron and hole densities when their quasi-Fermi levels coincide with the defect level. Before irradiation τ_{no} and τ_{po} are assumed to be 4.9×10^{-9} s and 2×10^{-8} s respectively [18]. Defects due to irradiation are presented in Table 1. The density of each defect is obtained by multiplying the introduction rate of the defect (k (cm^{-1})) by the electron fluence (Φ (cm^{-2})).

$U_{rd}(x)$ and $U_{Aug}(x)$ are, respectively, given by [19]:

$$U_{rd} = B\left(np - n_i^2\right) \tag{7}$$

$$U_{Aug} = (C_{nAu}n + C_{pAu}p)\left(np - n_i^2\right) \tag{8}$$

where $B = 7 \times 10^{-10}$ cm^3 s^{-1} and $C_{n,pAu} = 10^{-30}$ cm^6 s^{-1} [20].

For general ohmic contacts the surface recombination velocities for electron, S_n, and for holes, S_p, determine the carrier concentration at the boundaries. The electron and hole current densities for this type of contact are given by [14]:

$$J_n(0) = qS_n(n(0) - n_{eq}) \tag{9.a}$$

$$J_p(0) = qS_p(p(0) - p_{eq}) \tag{9.b}$$

$$J_n(d) = qS_n(n(d) - n_{eq}) \tag{9.c}$$

$$J_p(d) = qS_p(p(d) - p_{eq}) \tag{9.d}$$

n_{eq} and p_{eq} are the equilibrium electron and hole densities respectively and d is the sample thickness.

Table 1
Parameters of electron (E_i) and hole traps (H_i) induced in GaAs by electron irradiation from [4,8]; k is the introduction rate of defects, E_t the defect level position, σ_n and σ_p the capture cross-sections for electrons and holes, respectively.

Defects [4,9]	k (cm^{-1}) (defect introduction rate)	$E_C - E_T$ (eV)	σ_n (cm^2)
E_1	1.50	0.045	2.2×10^{-15}
E_2	1.50	0.140	1.2×10^{-13}
E_3	0.40	0.300	6.2×10^{-15}
E_4	0.08	0.760	3.1×10^{-14}
E_5	0.10	0.960	1.9×10^{-12}
Defects [4,8]	k (cm^{-1}) (defect introduction rate)	$E_T - E_V$ (eV)	σ_p (cm^2)
H_0	0.8	0.06	1.6×10^{-16}
H_1	0.1–0.7 (assumed 0.4 in this work)	0.29	5.0×10^{-15}
H_2	Not given (assumed 0.1 in this work)	0.41	2.0×10^{-16}
H_3	0.2	0.71	1.2×10^{-14}
τ_{no}	Electron lifetime before irradiation (s)		4.5×10^{-9} [18]
τ_{po}	Hole lifetime before irradiation (s)		2×10^{-8} [18]
v_{th}	Carrier thermal velocity (cm s^{-1})		10^7
B	Direct recombination coefficient (cm^3 s^{-1})		7×10^{-10} [20]
$C_{Aun(p)}$	Auger recombination coefficient (cm^6 s^{-1})		10^{-30} [20]

**Table 2**
The solar cell parameters used in the simulation.

| Symbol	Parameter	Value
E_g	Energy gap (eV)	$1.425 + 1.247x$, $x < 0.45$ [29]
χ	Electronic affinity (eV)	$4.07 - 1.1x$, $x < 0.45$ [29]
ε_r	Relative dielectric constant (F cm^{-1})	$13.18 - 3.12x$ [29]
T	Temperature (K)	300
N_A, d_p	p$^+$-layer doping (cm^{-3}) and thickness (μm)	$2 \times 10^{18}/4 \times 10^{17}$, 0.53
N_D, d_n	n$^+$-layer doping (cm^{-3}) and thickness (μm)	2×10^{17}, 0.5
	n-base doping (cm^{-3}) and thickness (μm)	10^{16}, 2.97
μ_n	Electron drift mobility (cm^2 V^{-1} s^{-1})	
	AlGaAs (undoped)	$8500 - 22{,}000x + 10^4x^2$, $x < 0.45$ [29]
	p$^+$-AlGaAs (assumed)	$(8500 - 22{,}000x + 10^4x^2)/2$
	p$^+$ GaAs	3000 [30]
	n-GaAs	8800 [21,30]
	n$^+$-GaAs	4000 [30]
μ_p	Hole drift mobility (cm^2 V^{-1} s^{-1})	
	AlGaAs (undoped)	$400 - 970x + 740x^2$, $x < 0.45$ [29]
	p$^+$-AlGaAs (assumed)	$(400 - 970x + 740x^2)/2$, $x < 0.45$
	p$^+$ GaAs	200 [30]
	n-GaAs	400 [21,30]
	n$^+$-GaAs	220 [30]
S_n	Electron surface recombination velocity (cm s^{-1})	10^4 [24]
S_p	Hole surface recombination velocity (cm s^{-1})	10^4 [24]
N_c	Effective density of states at E_c (cm^{-3})	2.5×10^{19} $(m_e^*/m_e)^{3/2}$ [31]
N_v	Effective density of states at E_v (cm^{-3})	2.5×10^{19} $(m_h^*/m_e)^{3/2}$ [31]
m_e^*/m_e	Effective electron mass/ electron mass	$0.067 + 0.083x$ [29]
m_h^*/m_e	Effective hole mass/ electron mass	$0.62 + 0.14x$ [29]
R_M	n/metal contact reflectivity (assumed)	0.95

The potential boundary conditions are:

$$\psi(0) = V_{app} \quad \text{and} \quad \psi(d) = V_d \tag{10}$$

where V_{app} is the applied voltage and V_d is the diffusion voltage calculated for variable composition by:

$$V_d = \frac{1}{q}(\chi(0) - \chi(d)) + \frac{k_B T}{q} \ln \frac{n(d)}{n(0)} \frac{N_c(0)}{N_c(d)} \tag{11}$$
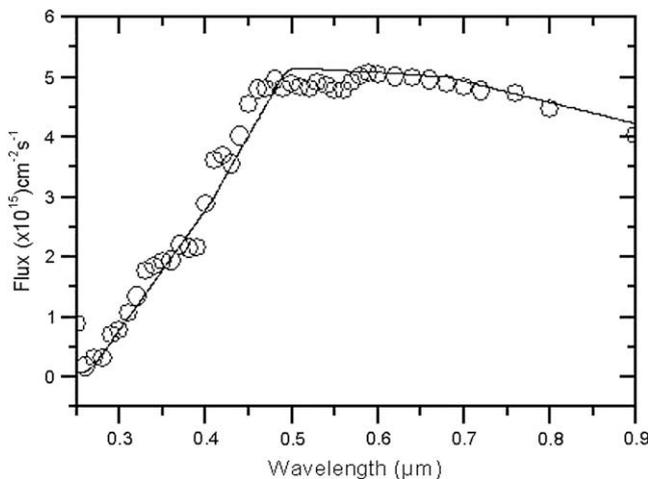
Fig. 1. The tabulated (symbols) [23] and fitted (solid line) fluxes of the AM0 spectrum.
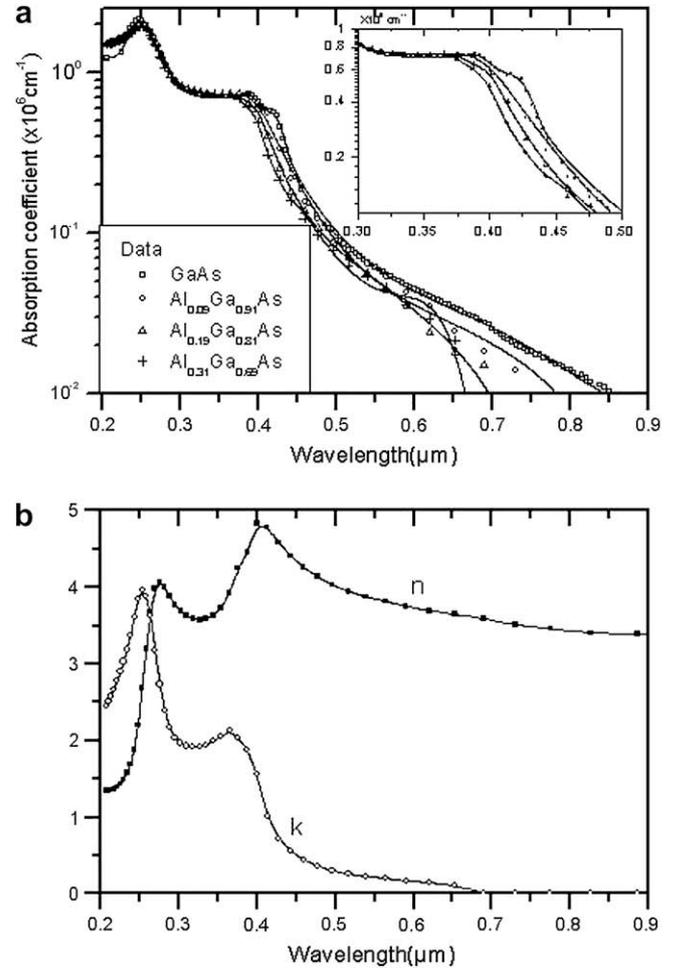
Fig. 2. The fitted and tabulated (a) absorption coefficient, (b) refractive index and extinction coefficient of the Al$_{0.31}$Ga$_{0.69}$As window.

The material parameters used in this simulation are presented in Table 2.

In order to study the effect of the AlGaAs window two cells with different window structures have been used. Both cells have (Al$_x$Ga$_{1-x}$As/GaAs)-p$^+$ type window/emitter, and n$^+$-type collector layers which are 0.53 and 0.5 μm thick, respectively, while the thickness of the n-type base region is 2.97 μm. For the first cell (Cell 1), the window is Al$_{0.31}$Ga$_{0.69}$As with a thickness of 0.03 μm while for the second cell (Cell 2), the window is Al$_{0.31}$Ga$_{0.69}$As/Al$_{0.19}$Ga$_{0.81}$As/Al$_{0.1}$Ga$_{0.9}$As with a total thickness of 0.09 μm (each layer is 0.03 μm thick). The doping densities of the different regions are: 2×10^{18} cm^{-3} for the Al$_x$Ga$_{1-x}$As-p$^+$ type window, 4×10^{17} cm^{-3} for the GaAs-p$^+$ type emitter, 1×10^{16} cm^{-3} for the n-type GaAs base and 2×10^{17} cm^{-3} for the n$^+$-type GaAs collector.

3. Optical parameters fitting

The cell's top surface is subjected to AM0 illumination with a power density of 135.6 W/cm^2 [19]. Light penetrates and is absorbed all along the structure and produces electron–hole pairs. The generation rate of these pairs at a position x from the illuminated front is given by [14]:

$$G(x) = \int_{Spectrum} T(\lambda)\phi_o(\lambda)\alpha(\lambda)[\exp(-\alpha(\lambda)x) + R_B \exp(-\alpha(\lambda)(2d - x))]d\lambda \tag{12}$$

Table 3
Parameters of Cell Ref [11] used to check the 1 MeV electron irradiation defect parameters. The p$^+$ contact and the n substrate are modelled as limit conditions.

Layer	Doping (cm^{-3})	Thickness (μm)
p$^+$/n cell		
p$^+$ contact	1×10^{19}	0.18
Al$_{0.85}$Ga$_{0.15}$As window	2×10^{18}	0.03
p emitter	3.85×10^{17}	0.48
n-base	3.40×10^{16}	2.85
n$^+$ buffer	3.12×10^{17}	0.54
n substrate	4.52×10^{18}	N/A

Table 4
Capture cross-sections used to obtain the best fitting to experimental measurements in [11] of the short current density degradation for 1 MeV electron irradiation.

Defects [4,8]	σ_n (cm^2)	σ_n/σ_p
E_2	5.0×10^{-13}	100
E_3	5.0×10^{-14}	100
E_4	3.1×10^{-13}	100
E_5	3×10^{-11}	100
Defects [4,8]	σ_p (cm^2)	σ_p/σ_n
H_1	5.0×10^{-14}	100
H_2	1.0×10^{-15}	100
H_3	1.0×10^{-13}	100

In (12), $T(\lambda)$ is the transmittance of the cell's top surface (AlGaAs window), calculated for normal incidence by [21]:

$$T(\lambda) = 1 - R(\lambda) = 1 - \frac{(n(\lambda) - 1)^2 + k(\lambda)^2}{(n(\lambda) + 1)^2 + k(\lambda)^2} \tag{13}$$

where $R(\lambda)$ is the reflectivity, $n(\lambda)$ and $k(\lambda)$ are, respectively, the refractive index and the extinction coefficient of the AlGaAs window.

$\phi_o(\lambda)$ is the AM0 spectrum flux, $\alpha(\lambda)$ is the absorption coefficient which depends on the layer composition. The back reflection is taken into account by introducing the back reflectivity R_B in (12).

The quantities $\phi_o(\lambda)$, $\alpha(\lambda)$, $n(\lambda)$ and $k(\lambda)$ are given in a tabulated form in research papers and text books [22,23] for non-uniform variations of the wavelength. However for the purpose of numerical simulation all these quantities have to be calculated in the same range as well as the same variations of the wavelengths and a fitting procedure is useful to produce this.

The AM0 spectrum flux is fitted to an expression of the form, similar to that of [24] for AM1.5 spectrum flux, thus:

$$\phi_o \left(\times 10^{15}\,\mathrm{cm}^{-2}\mathrm{s}^{-1} \right) = \begin{cases} 20\lambda - 5 & 0.26 \leq \lambda(\mu m) < 0.4 \\ 25.1\lambda - 7 & 0.4 \leq \lambda(\mu m) < 0.5 \\ -0.808\lambda + 5.555 & 0.5 \leq \lambda(\mu m) < 0.68 \\ -3.535\lambda + 7.373 & 0.68 \leq \lambda(\mu m) \leq 0.9 \end{cases} \tag{14}$$

The fitted flux is compared to the tabulated flux in Fig. 1.

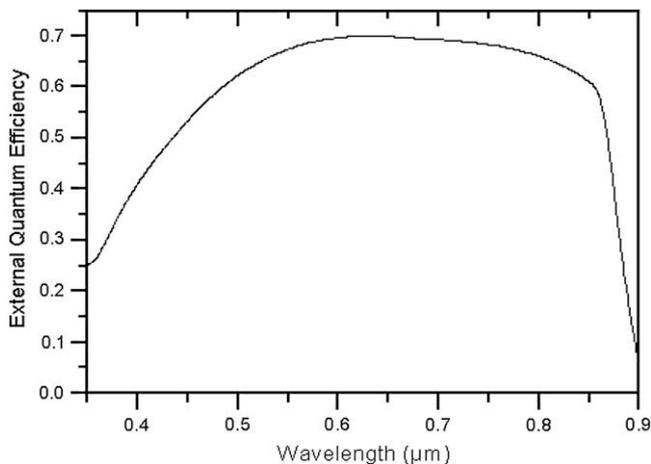However for $\alpha(\lambda)$, $n(\lambda)$ and $k(\lambda)$, there are no equivalent to (14) in the literature so the whole range of wavelength is divided into several segments to find a best fit equation for each segment. The obtained expressions are very long and complex to be presented here. The fitted $\alpha(\lambda)$ is presented in Fig. 2(a) for the different AlGaAs compositions used in this work. Fig. 2(b) shows the $n(\lambda)$ and $k(\lambda)$ data and fitting for the Al$_{0.31}$Ga$_{0.69}$As window.

4. Results and discussion

In order to check the reliability of our in-house developed program, a solar cell structure used in an experimental work [11] was simulated. The simulated structure is a p$^+$/n NRL cell (called hereafter Cell Ref) for which the parameters are given in Table 3. The illuminated current–voltage measurements were performed under 1 sun AM0 (1367 W/m^2) conditions at 25 °C using an Oriel 1000 W solar simulator and the cell did not have an antireflective coating.

In Fig. 3 the calculated pre-irradiation external quantum efficiency ($J_{sc}(\lambda)/\phi_o(\lambda)$) is presented. It was found to be in a good agreement with that of [11]. The average pre-irradiation values for the photocurrent, photovoltage and efficiency were 22.87 mA cm^{-2}, 0.949 V and 13.19% [11] while our simulated photocurrent, photovoltage and efficiency are, respectively, 24.1 mA cm^{-2}, 1.00 V and 15.60%. The slight difference between simulated and experimental results may be due to a possible difference between illumination conditions.

For the irradiated structure and as mentioned before in the numerical model section, the irradiation effect is modelled by introducing energy levels in the GaAs gap (see Table 1). Unfortunately by using these parameters the simulation did not reproduce the observed irradiation effect of the 1 MeV electron dose of [11].
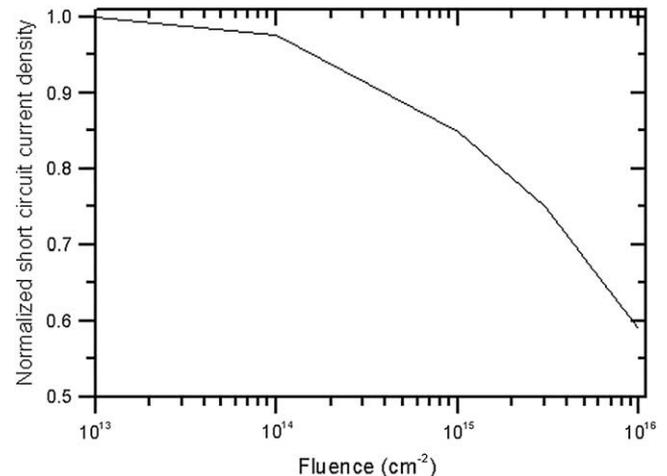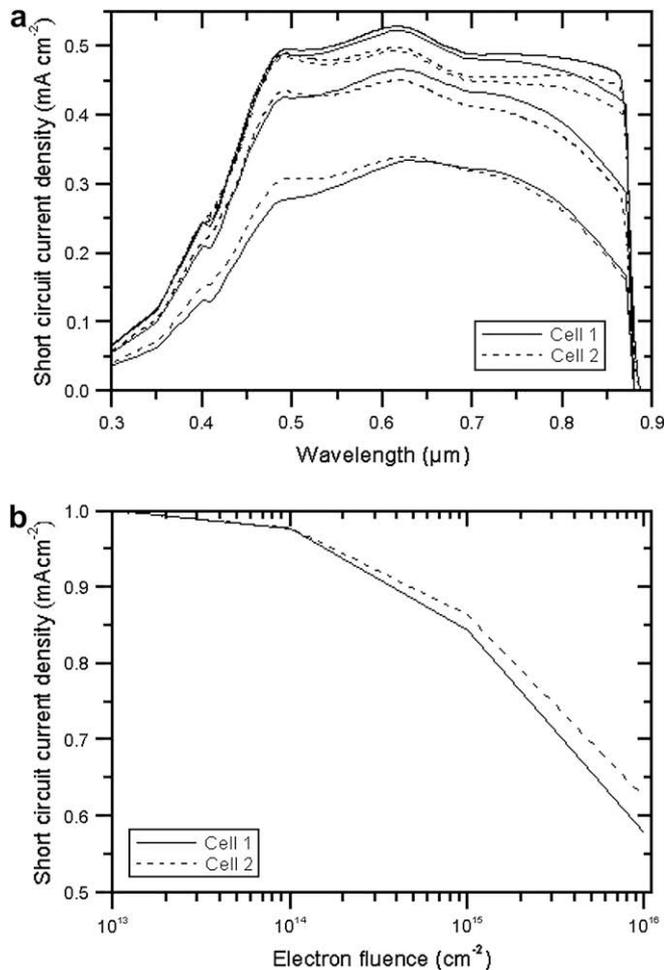

Fig. 3. The simulated external quantum efficiency for Cell Ref before irradiation.

Fig. 4. The simulated short circuit current density degradation by 1 MeV electron irradiation (normalised) for Cell Ref.
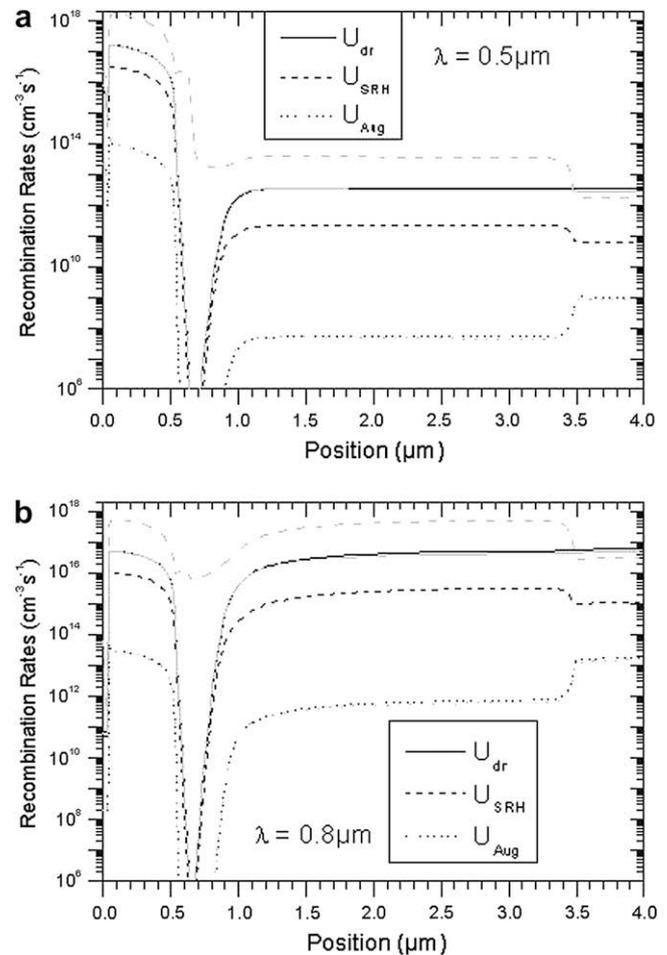
Fig. 5. (a) Degradation of the spectral response by the different electron fluences ($\Phi = 10^{14}$, 10^{15} and 10^{16} cm^{-2}) for the Al$_{0.31}$Ga$_{0.69}$As–p$^+$ (0.03 μm)/GaAs–p$^+$–n–n$^+$ solar cell (solid lines) and for the gradual AlGaAs–p$^+$ (0.1 μm)/GaAs–p$^+$–n–n$^+$ solar cell (dashed lines), (b) the corresponding short circuit current density degradations.

Fig. 6. Recombination rates before and after irradiation for $\Phi = 10^{14}$ cm^{-2}, (a) $\lambda = 0.5$ μm and (b) $\lambda = 0.8$ μm.

A possible explanation of this is that it is a well-known fact that there are big uncertainties in evaluating the parameters of defects especially when a large number of them are present in a sample such as an irradiated GaAs solar cell. Therefore an adjustment of the capture cross-sections of Table 1 (except for E_0 and H_1) is made in order to obtain a good fit of the irradiation effect on the short circuit current. The required capture cross-section values, for a good fit of simulation to experimental results, are given in Table 4 and the simulated degraded short circuit current density of the cell reference is shown in Fig. 4 which is in agreement with experimental data of [11].

These capture cross-sections are then used to predict the defect effect on the solar cells considered in this work (Cell 1 and Cell 2). These cells differ from Cell Ref in the fact that the first absorbent layer is an AlGaAs window. This allows a clear study of the effect of its thickness and composition on the cell's light absorption and consequently the resulting spectral response. However with a p$^+$ layer contact thick enough (0.2 μm), as used in Cell Ref, it is certain that the most important absorption occurs in the GaAs layer and consequently the AlGaAs layer absorption will have no noticeable effect on the cell spectral response.

First, the current–voltage characteristics and the spectral response of the illuminated cells (Cell 1 and Cell 2) before irradiation are calculated. The extracted photocurrent, photovoltage, fill factor and efficiency are, respectively, $J_{sc} = 24.0$ mA cm^{-2}, $V_{oc} = 1.01$ V, $FF = 0.88$, and $\eta = 15.65\%$ for Cell 1, and $J_{sc} = 23.0$ mA cm^{-2}, $V_{oc} = 1.01$ V, $FF = 0.88$, and $\eta = 15.00\%$ for Cell 2. These values are fairly in agreement with standard values for such cells [11,25–27]. The spectral responses obtained for both cells are presented in Fig. 5(a). The spectral response of Cell 2 is inferior to that of Cell 1 between 0.5 and 0.85 μm. This is expected since absorption occurs mainly in the AlGaAs window for Cell 2 and the GaAs emitter for Cell 1 and as shown in Fig. 2 the absorption coefficient of AlGaAs is smaller than that of GaAs in the most efficient region of the AM0 spectrum.

The effect of the electron irradiation on Cell 1 and Cell 2 spectral responses is also presented in Fig. 5(a). For the $\Phi = 10^{14}$ cm^{-2} electron fluence, the degradation is more pronounced between 0.75 and 0.9 μm. For $\Phi = 10^{15}$ cm^{-2} and $\Phi = 10^{16}$ cm^{-2} the irradiation effect is over the whole wavelength range. These observations are fairly in agreement with measurement and simulation in [18,25] although the used cell's structure and defect levels are different. An attempt to explain this is given later on the basis on the recombination rates at wavelengths of interest.

By comparing the irradiation effect on Cell 1 and Cell 2, it was found that the gradual AlGaAs window improves the resistance of the spectral response for the short wavelength although the initial one (before irradiation) is poorer. This is more clarified in Fig. 5(b) which shows the degradation of the normalised short current densities for the two cells. For both cells the degradations are in the experimental range [11,18,28]. Cell 2 shows better resistance to electron irradiation due to the fact that deep levels are more effective in GaAs which has smaller energy gap than AlGaAs.

In the end an explanation of the electron irradiation effect using the different recombination rates variation with irradiation fluence is attempted. In Fig. 6(a) and (b) the recombination rates for Cell 1 for example, before and after irradiation ($\Phi = 10^{14}$ cm^{-2}) for two wavelengths (0.5 and 0.8 μm) are plotted. Before irradiation and for $\lambda = 0.5$ μm, the direct recombination is dominant. For $\lambda = 0.8$ μm there is an important increase in all recombination rates and the direct recombination stills dominant. After irradiation, for both $\lambda = 0.5$ and 0.8 μm, the SRH recombination becomes dominant while the other recombination rates are practically unaffected. The more sensitivity of the spectral response at $\lambda = 0.8$ μm is due then to the important increase of the SRH recombination. Evidently for $\Phi = 10^{15}$ and 10^{16} cm^{-2} the increase of the SRH recombination rate is more important.

5. Conclusion

Previous studies on the irradiation-induced defects have shown that it is very difficult to characterise their nature, densities and energy levels. This work constitutes a contribution to reach this aim by adjusting some of the defects parameters so that the numerical simulation fits experimental observations. A one-dimensional modelling of an AlGaAs-p$^+$/GaAs-(p$^+$–n–n$^+$) solar cell operating under AM0 solar spectrum and exposed to 1 MeV electron irradiation is presented. A comparison with experimental measurements [12] is made to check the reliability of the parameters simulation (mainly the irradiation defects parameters). Our simulation program reproduces well the 1 MeV electron irradiation degradation of the short circuit current density of [11] using defects energy levels given by Bourgoin et al. [4,8] but with different capture cross-sections. The adjusted parameters are then used in the simulation to study the effect of the Al molar fraction and thickness of the AlGaAs window on the cell sensitivity to the electron irradiation-induced defects. It was found that the use of a gradual energy gaps Al$_x$Ga$_{1-x}$As window improves the resistance of the cell's spectral response at short wavelengths. Experimental validation of the theory is desirable.

References

[1] Yamaguchi M. Radiation-resistant solar cells for space use. Solar Energy Materials & Solar Cells 2001;68:31–53.
[2] Bourgoin JC, de Angelis N. Radiation-induced defects in solar cell materials. Solar Energy Materials & Solar Cells 2001;66:467–77.
[3] de Angelis N, Bourgoin JC, Takamoto T, Khan A, Yamaguchi M. Solar cell degradation by electron irradiation. Comparison between Si, GaAs and GaInP cells. Solar Energy Materials & Solar Cells 2001;66:495–500.
[4] Bourgoin JC, Zazoui M. Irradiation-induced degradation in solar cell: characterisation of recombination centres. Semiconductor Science and Technology 2002;17:453–60.
[5] Hovel HJ, Woodall JM. Ga$_{1-x}$Al$_x$As–GaAs P–N–N heterojunction solar cells. Journal of Electrochemical Society 1973;120:1246.
[6] Sutherland JE, Hauser JR. IEEE Transactions on Electron Devices 1977;ED 24(4):363.
[7] Usami A, Hamamoto Y, Sonobe M. A computer analysis of Ga$_{1-x}$Al$_x$GaAs solar cell with multilayered window structure. IEEE Transactions on Electron Devices 1978;ED 25(5):546.
[8] Pons D, Bourgoin JC. Irradiation-induced defects in GaAs. Journal of Physics C: Solid State Physics 1985;18:3839–71.
[9] Mbarki M, Sun GC, Bourgoin JC. Prediction of solar cell degradation in space from the electron–proton equivalence. Semiconductor Science and Technology 2004;19:1081–5.
[10] Hadrami M, Roubi L, Zazoui M, Bourgoin JC. Relation between solar cell parameters and space degradation. Solar Energy Materials & Solar Cells 2006;90:1486–97.
[11] Warner JH, Messenger SR, Walters RJ, Summers GP, Lorentzen JR, Wilt DM. Correlation of electron radiation induced-damage in GaAs solar cells. IEEE Transactions on Nuclear Science 2006;53(4):1988–94.
[12] Meftah AF, Sengouga N, Belghachi A, Meftah AM. Numerical simulation of the effect of recombination centres and traps created by electron irradiation on the performance degradation of GaAs solar cells. Journal of Physics C: Condensed Matter, in press.
[13] Kurata M. Numerical analysis for semiconductor devices. Lexington, MA: Heath; 1982.
[14] Zeman M, van den Heuvel J, Kroon M, Willemen J. Amorphous semiconductor analysis (ASA) user's manual. Version 3.3. Delft, The Netherlands: Delft University of Technology; 2000.
[15] Miller GL, Lang DV, Kimerling LC. In: Hungings RA, Bube RH, Roberts RW, editors. Annual review of materials science; 1977. p. 377–448.
[16] Schockley W, Read WT. Statistics of the recombination of holes and electrons. Physical Review 1952;87:835.
[17] Hall RN. Electron–hole recombination in germanium. Physical Review 1952;87:387.
[18] Crespin AL. A novel approach to modeling the effect of radiation in gallium–arsenide solar cells using Silvaco's Atlas software. Master thesis, Monterey, CA: Naval Postgraduate School; 2004.
[19] Würfel P. Physics of solar cells, from principles to new concepts. Wiley-VCH; 2005.
[20] http://www.ioffe.ru/SVA.
[21] Sze SM. Physics of semiconductor devices. 2nd ed. New York: John Wiley and Sons; 1982.
[22] Eque B. Energie solaire photovoltaique, Tome 1: Physique et technologie de la conversion photovoltaique. Paris: Ellipses, UNESCO; 1993.
[23] Adachi S. Properties of aluminium gallium arsenide. INSPEC; 1993.
[24] Liou JJ, Wong WW. Comparison and optimization of the performance of Si and GaAs solar cells. Solar Energy Materials & Solar Cells 1992;28:9.
[25] Michael S. A novel approach for the modelling of advanced photovoltaic devices using the SILVACO/ATLAS virtual wafer fabrication tools. Solar Energy Materials & Solar Cells 2005;87:771.
[26] Green MA, Emery K, King DL, Igari S, Warta W. Solar cell efficiency tables (version 21). Progress in Photovoltaics: Research and Applications 2003;11:39–45.
[27] Chandrasekaran N, Soga T, Inuzuka Y, Imaizumi M, Taguchi H, Jimbo T. 1 MeV electron irradiation effects of GaAs/Si solar cells. Materials Research Society Symposium Proceedings 2005;836:L6.7.1–6.7.6.
[28] Loo RY, Kamath GS, Li SS. Radiation damage and annealing in GaAs solar cells. IEEE Transactions on Electron Devices 1990;37(2):485.
[29] Adachi S. GaAs, AlAs and Al$_x$Ga$_{1-x}$As: material parameters for use in research and device applications. Journal of Applied Physics 1985;58(3):R1–29.
[30] Neamen DA. Semiconductor physics and devices, basic principles. 3rd ed. McGraw Hill; 2003.
[31] Mathieu H. Physique des semiconducteurs et des composants électroniques. 3rd ed. Paris: Masson; 1996.